



**HAL**  
open science

## Selective Homonuclear Hartmann-Hahn for $^{13}\text{C}$ $\rightarrow$ $^{13}\text{C}$ Polarization Transfer in Solution State NMR

Thomas Eykyn, Martin O Leach

► **To cite this version:**

Thomas Eykyn, Martin O Leach. Selective Homonuclear Hartmann-Hahn for  $^{13}\text{C}$   $\rightarrow$   $^{13}\text{C}$  Polarization Transfer in Solution State NMR. *Molecular Physics*, 2007, 105 (13-14), pp.1827-1832. 10.1080/00268970701420532 . hal-00513106

**HAL Id: hal-00513106**

**<https://hal.science/hal-00513106>**

Submitted on 1 Sep 2010

**HAL** is a multi-disciplinary open access archive for the deposit and dissemination of scientific research documents, whether they are published or not. The documents may come from teaching and research institutions in France or abroad, or from public or private research centers.

L'archive ouverte pluridisciplinaire **HAL**, est destinée au dépôt et à la diffusion de documents scientifiques de niveau recherche, publiés ou non, émanant des établissements d'enseignement et de recherche français ou étrangers, des laboratoires publics ou privés.



**Selective Homonuclear Hartmann-Hahn for  $^{13}\text{C} \rightarrow ^{13}\text{C}$   
Polarization Transfer in Solution State NMR**

|                               |  |
|-------------------------------|--|
| Journal:                      | <i>Molecular Physics</i>   |
| Manuscript ID:                | TMPh-2007-0087.R1  |
| Manuscript Type:              | Research Note  |
| Date Submitted by the Author: | 20-Apr-2007  |
| Complete List of Authors:     | Eykyn, Thomas; The Institute of Cancer Research, Cancer Research UK Clinical Magnetic Resonance Group<br>Leach, Martin; The Institute of Cancer Research, Cancer Research UK Clinical Magnetic Resonance Group |
| Keywords:                     | NMR, polarization transfer, dynamic nuclear polarization, $^{13}\text{C}$ , homonuclear Hartmann-Hahn  |
|                               |  |



1  
2  
3  
4  
5  
6  
7  
8  
9  
10  
11  
12  
13  
14  
15  
16  
17  
18 **Selective Homonuclear Hartmann-Hahn for  $^{13}\text{C}$   $\rightarrow$   $^{13}\text{C}$  Polarization Transfer in**  
19 **Solution State NMR**  
20  
21  
22  
23  
24

25 Thomas R. Eykyn<sup>†</sup>, Martin O. Leach  
26  
27  
28  
29  
30  
31  
32

33 Ref 0703P  
34  
35  
36  
37  
38  
39  
40  
41  
42  
43  
44  
45  
46  
47  
48  
49  
50  
51  
52

40 Cancer Research UK Clinical Magnetic Resonance Research Group, The Institute of  
41  
42 Cancer Research, Royal Marsden Foundation NHS, Downs Rd.  
43  
44 Sutton, Surrey, SM2 5PT. United Kingdom.  
45  
46  
47  
48  
49  
50  
51  
52

53 <sup>†</sup> Author to whom correspondence should be addressed  
54

55 Email: thomas.eykyn@icr.ac.uk  
56

57 Tel: +44 20 8661 3390  
58

59 Fax: +44 20 8661 0846  
60

**ABSTRACT**

Polarization transfer has become a commonplace technique for the enhancement of a variety of nuclei in high field nuclear magnetic resonance (NMR). In this paper we re-visit the homonuclear Hartmann-Hahn method for polarization transfer and show that a 90% transfer of polarization can be achieved experimentally between a pair of scalar coupled  $^{13}\text{C}$  nuclei in a sample of isotopically enriched glycine. This may show particular utility in the field of dynamic nuclear polarization (DNP) and could be used as an addendum to already established DNP techniques allowing the favourable enhancement to be 'stored' on long-lived nuclei and subsequently transferred to shorter-lived nuclei prior to observation.

**Key Words:** NMR, polarization transfer, dynamic nuclear polarization,  $^{13}\text{C}$ , homonuclear Hartmann-Hahn.

## I. INTRODUCTION

Hyperpolarization methods are becoming an invaluable way to enhance the intrinsic signal achieved by NMR and thereby extend the range of possible applications. These techniques rely on generating non-equilibrium populations of nuclear spin-states. A number of conceptually related methods have shown utility for generating hyperpolarized species such as brute-force polarization [1], optical pumping of noble gases [2-4], para-hydrogen induced polarization (PHIP) [5] and Dynamic Nuclear Polarization (DNP) [6,7]. The most general of these methods is DNP where the polarization is generated by microwave irradiation of un-paired electrons in a free radical and subsequent transfer of electron polarization to nuclear polarization in the solid state at temperatures below 4K. Recent advances have made it possible to dissolve the polarised solid sample in a room temperature solvent whilst retaining the generated polarization. These have made the DNP technique amenable to a variety of solution state NMR techniques, not least in biological systems. Dynamic nuclear polarization has been shown to enhance the nuclear polarization of  $^{13}\text{C}$  in a variety of small organic molecules to levels in excess of 10,000 [8]. Potential applications for this technique include molecular imaging of endogenous substrates [9] and real time metabolic imaging with applications to diagnostic MR in oncology [10,11].

The DNP technique is found to be most efficient for long  $T_1$  nuclei such as carbonyl or quaternary  $^{13}\text{C}$  largely due to limitations imposed by the dissolution and transfer steps. A number of methods may be subsequently used to transfer coherence from nuclei that have a favourable enhancement to those that are less favourable. Laboratory frame techniques such as INEPT [12] have shown great utility in the solution state whereas rotating frame experiments such as cross-polarization [13] have been more widely used for solid-state experiments. Selective cross-polarization techniques have recently been shown to be a highly efficient method for achieving heteronuclear polarization transfer between spin  $\frac{1}{2}$  nuclei in solution state [14,15] and is also applicable to scalar coupled quadrupolar spin systems [16,17]. This has been applied to selective excitation in isotopically labelled biomolecules [18]. The homonuclear variant of this method has been applied to proteins and peptides [19] and has shown recent application for *in vivo* spectral editing of endogenous metabolites such as  $\gamma$ -aminobutyric acid (GABA) in the human brain at 3T [20].

In this paper we consider the possibility of transferring polarization between two scalar coupled  $^{13}\text{C}$  nuclei in solution state by selective cross-polarization and show that at least a 90% transfer of polarization can be achieved in a sample of  $^{13}\text{C}$  labelled glycine. The method is straightforward to implement and may show particular utility with the advent of novel applications in DNP.

## II. HOMONUCLEAR HARTMANN-HAHN

We first outline the analytical procedures for calculating the transfer functions for cross-polarization between two scalar-coupled spins  $S = 1/2$ . The theory and methodology are analogous to that previously developed for  $^1\text{H}$ - $^1\text{H}$  homonuclear coherence transfer [19]. We here assume  $S$  to be  $^{13}\text{C}$  although the method is general for other scalar coupled homonuclear systems. Throughout the following discussion relaxation will be neglected.

One of the major limitations for achieving homonuclear coherence transfer between  $^{13}\text{C}$  nuclei by conventional cross-polarization is the large chemical shift range. Consequently resonance frequencies may be several kHz apart requiring the use of high power RF to cover the entire chemical shift range. This may lead to potential problems with overheating and power deposition when applying long RF pulses. To circumvent this problem we propose using a doubly selective spin-locking pulse that is resonant with the two  $^{13}\text{C}$  nuclei. This is achieved by modulating the amplitude of a square pulse with the function  $\cos(\Delta\Omega t)$  where  $\Delta\Omega = 1/2(\Omega_1 - \Omega_2)$  and applying the carrier of the spin-locking field midway between the two frequencies. This modulation causes the response of the spin-lock field to be split into two side bands at  $\omega_0 \pm \Delta\Omega$  which will be resonant with the two chemical shifts. One clear advantage of homonuclear coherence transfer over its heteronuclear counterpart is that there is no need to calibrate the Hartmann-Hahn condition since the same transmitter coil generates the two fields.

Assuming that the transmitter is positioned midway between the two chemical shifts then the Hamiltonian may be written in the rotating frame as [19]

$$H(t) = 2\omega_1 \cos(\Delta\Omega t)(S_{1x} + S_{2x}) + \Delta\Omega(S_{1z} - S_{2z}) + 2\pi J_{12}S_{1z}S_{2z}. \quad (1)$$

It has been shown [21] that the density operator ( $\sigma$ ) may be re-cast into the doubly rotating frame (DR) employing the unitary transformation  $\sigma^{\text{DR}}(t) = U\sigma(t)U^{-1}$  where  $U = \exp(-i\Delta\Omega t(S_{1z} - S_{2z}))$ . In the presence of two RF fields that are on-resonance for the selected spins  $S_1$  and  $S_2$ , the Hamiltonian in the doubly rotating frame becomes time-independent and may be written as

$$H = \omega_1 S_{1x} + \omega_1 S_{2x} + 2\pi J_{12} S_{1z} S_{2z}. \quad (2)$$

where the RF amplitude is given by  $\omega_1 = -\gamma^S B_1^S$  and the scalar-coupling constant is given by  $J_{12}$ . For a two-spin system the above Hamiltonian is given by a 4 x 4 matrix and may be calculated using standard product operator formulism.

Coherence transfer functions can be derived for initial and final operators  $A$  and  $B$  given by,  $\langle B \rangle = \text{Tr}\{U(\tau)AU^{-1}(\tau)B\}$  where the propagator ( $U$ ) is given by  $U(\tau) = \exp(-iH\tau)$ . In the case where the sum of the RF field strengths is greater than the scalar coupling,  $2\omega_1 \gg \pi J$ , an analytical solution is readily derived. For an initial density operator  $\sigma(0) = S_{1x}$ , corresponding to transverse magnetization on spin 1, the evolution is given by

$$\langle S_{1x} \rangle(\tau) = \frac{1}{2}(1 + \cos(\pi J\tau)), \quad (3a)$$

$$\langle 2S_{1y}S_{2z} \rangle(\tau) = \frac{1}{2}\sin(\pi J\tau), \quad (3b)$$

$$\langle 2S_{1z}S_{2y} \rangle(\tau) = -\frac{1}{2}\sin(\pi J\tau), \quad (3c)$$

$$\langle S_{2x} \rangle(\tau) = \frac{1}{2}(1 - \cos(\pi J\tau)). \quad (3d)$$

Equations 3(a) and (b) correspond to in-phase and antiphase coherences of the source spin 1 while equations 3(c) and (d) correspond to antiphase and in-phase coherences of the destination spin 2. A maximum transfer to spin 2 occurs for a spin-lock duration of  $\tau = 1/J$ . This is in contrast to homonuclear TOCSY type experiments where the maximum transfer occurs for a contact time of  $\tau = 1/2J$ .

### III. INFLUENCE OF HETERONUCLEAR SCALAR COUPLING TO $^1\text{H}$

The presence of additional scalar couplings to passive spins is known to adversely affect the efficiency of Hartmann-Hahn methods [22]. Homonuclear coherence transfer between  $^{13}\text{C}$  nuclei presents additional challenges, notably  $^{13}\text{C}$  nuclei invariably possess one or more directly bound protons with a large one-bond heteronuclear scalar coupling constant of the order  $^1J_{\text{HC}} \approx 140$  Hz. This is nearly three times larger than a typical  $^1J_{\text{CC}} \approx 55$  Hz and therefore has the potential to dominate the evolution of the spin-system under selective spin-locking fields. Furthermore additional two and three bond couplings may also be present. We extend the theory above to include the presence of these additional couplings. The Hamiltonian in equation (2) may be extended using standard product operator formalism and may be written,

$$H^R = \omega_1 S_{1x} + \omega_1 S_{2x} + 2\pi J_{12} S_{1z} S_{2z} + 2\pi J_{23} S_{2z} I_{3z} + 2\pi J_{13} S_{1z} I_{3z}. \quad (4)$$

For a three-spin system the above Hamiltonian is given by an  $8 \times 8$  matrix. Numerical simulation has been employed to examine the effect these additional couplings may have on the mechanism of cross-polarization. Additional couplings may also be included in the above theory although a three spin system is adequate for the current purpose.

Figure 1 shows the transfer response of the  $^{13}\text{C}$  magnetization as a function of the spin-lock duration during the cross-polarization period either in the presence or absence of additional couplings to  $^1\text{H}$ . Coherence transfer functions are calculated employing the Hamiltonian in equation (4) and assuming a three spin system  $^{13}\text{C}$ - $^{13}\text{C}$ - $^1\text{H}$  where the scalar coupling constants were  $^1J_{\text{CC}} = 50$  Hz,  $^1J_{\text{CH}} = 145$  Hz and  $^2J_{\text{CH}} = 10$  Hz. All calculations assume an initial density operator  $\sigma(0) = S_{1x}$  corresponding to transverse magnetization on spin 1. The spin-lock amplitude was set equal to the scalar coupling constant  $\omega_1/2\pi = 50$  Hz. Figure 1(a) and (b) show coherence transfer curves as a function of the spin-lock duration  $\tau_{\text{CP}}$  where the additional scalar coupling to proton were turned off, i.e.  $^1J_{\text{CH}} = ^2J_{\text{CH}} = 0$  Hz. Figure 1(a) shows the expectation values of spin 1 coherences  $\langle S_{1x} \rangle$  and  $\langle 2S_{1y}S_{2z} \rangle$ , solid and dashed lines respectively, whilst figure 1(b) shows the expectation values of spin 2 coherences  $\langle S_{2x} \rangle$  and  $\langle 2S_{1z}S_{2y} \rangle$ , solid and dashed-dotted lines respectively. In this case the coupling



network reduces to a two-spin system and the transfer functions are identical to those derived from equation (2). If the RF amplitude is at least of the order of the scalar coupling constant then the method is efficient and gives rise to a maximum transfer for  $\tau_{CP} = 1/J_{CC} = 20$  ms. The mechanism of cross-polarization is mediated via anti-phase coherences and consequently an in-phase-to-in-phase coherence transfer will only be achieved for accurately calibrated spin-lock durations. Figures 1(c) and (d) show the same transfer functions but with the additional couplings to  $^1\text{H}$  turned on. Figure 1(c) shows the expectation values of spin 1 coherences  $\langle S_{1x} \rangle$  and  $\langle 2S_{1y}S_{2z} \rangle$ , solid and dashed lines respectively, whilst figure 1(d) shows the expectation values of spin 2 coherences  $\langle S_{2x} \rangle$  and  $\langle 2S_{1z}S_{2y} \rangle$ , solid and dashed-dotted lines respectively. One may note that evolution under the heteronuclear  $^1\text{H}$ - $^{13}\text{C}$  scalar couplings is highly detrimental to the method. Indeed for a spin-lock duration  $\tau_{CP} = 20$  ms and a weak spin-locking RF field strength no transfer of magnetization occurs. These simulations demonstrate the importance of decoupling the scalar coupling interactions to  $^1\text{H}$ .

#### IV. INFLUENCE OF SPIN-LOCK AMPLITUDE

To assess the influence of spin-lock amplitude on the efficiency of cross-polarization it is important to consider the nature of the cosine modulated RF field. Indeed generating two side bands in this manner is equivalent to applying two selective RF fields at the resonance frequencies of the two  $^{13}\text{C}$  nuclei of interest. There is a well-established interaction between two selective RF pulses when the two approach one another in the frequency domain [23]. When the RF amplitude becomes of the same order as the frequency difference between the two excitation regions then there is an inevitable interaction between the off-resonance field of one pulse with its neighbouring on-resonance field, thus disturbing the frequency response.

In figure 2 we consider, by way of simulation, the excitation region of a cosine modulated square RF pulse as a function of the offset from the carrier frequency. The pulse was a 10 ms pulse which was cosine modulated with a frequency  $\Delta\Omega = 1000$  Hz. The simulation displays the magnitude of the excited transverse magnetization  $(M_x^2 + M_y^2)^{1/2}$  at two different field strengths. In figure 2(a) the RF amplitude was  $\omega_1/2\pi = 50$  Hz, i.e. much smaller than the offset frequency of the cosine modulation. The response is split into two bands with minimal cross contamination between the two. Note that for low RF amplitudes the pulse yields the required response with

clean excitation bands at  $\pm 1000$  Hz. In figure 2(b) the RF amplitude was  $\omega_1/2\pi = 1000$  Hz which is equal to the offset difference of the cosine modulation. Note that the response is highly perturbed by 'cross-talk' between the two RF fields and the pulse no longer possesses clean excitation bands at  $\pm 1000$  Hz.

It is expected that RF fields of the type shown in figure 2(a) will be amenable to achieving coherence transfer by cross-polarization whereas the response shown in (b) will be highly detrimental to the mechanism of cross-polarization. These conclusions are further supported by experiment, see below.

## V. RESULTS

Figure 3 shows the pulse sequence that can be used to achieve cross-polarization between two spins  $S = {}^{13}\text{C}$ . A selective  $(\pi/2)_y$  Gaussian pulse is applied to one of the  ${}^{13}\text{C}$  nuclei and prepares an initial state of  $S_{Ix}$  transverse magnetization.

Experiments were carried out on a Bruker DRX 500 MHz spectrometer equipped with a BBO probe at 298 K. The sample employed was 100 mM uniformly enriched  ${}^{13}\text{C}$  glycine in  $\text{D}_2\text{O}$ . The scalar coupling constants were measured to be  ${}^1J_{\text{CC}} = 53.5$  Hz,  ${}^1J_{\text{CH}} = 143.8$  Hz and  ${}^2J_{\text{CH}} = 5.35$  Hz. The frequency separation between the two  ${}^{13}\text{C}$  resonances was 8226 Hz. The  $T_1$  relaxation times were measured by inversion recovery and found to be 28.4s for the carbonyl and 4.3s for the alpha carbon. All spectra were recorded with a relaxation delay of 150s to allow complete recovery to equilibrium.

Figure 4 shows experimental results of the integrated signal intensity as a function of the RF amplitude, of the alpha  ${}^{13}\text{C}$  following selective excitation of the carbonyl carbon and subsequent cross-polarization for a duration  $\tau_{\text{CP}} = 18.7$  ms. The vertical scale is given as a percentage of the integrated signal of the initial carbonyl carbon magnetization following selective excitation. **The solid line is a third order polynomial fit to guide the eye.** The maximum transfer of polarization was achieved when the RF amplitude is of the order  $\omega_1/2\pi \approx 200$  Hz. As one reduces the RF field strength then the transfer efficiency decreases, as the two components of the  ${}^{13}\text{C}$  doublets are not efficiently locked. Note also the detrimental effect of increasing the RF field strength. This is a consequence of the increasing cross talk between the side bands of the RF field, as shown in figure 2, and severely reduces the efficiency of cross-polarization.

1  
2  
3  
4  
5  
6  
7  
8  
9  
10  
11  
12  
13  
14  
15  
16  
17  
18  
19  
20  
21  
22  
23  
24  
25  
26  
27  
28  
29  
30  
31  
32  
33  
34  
35  
36  
37  
38  
39  
40  
41  
42  
43  
44  
45  
46  
47  
48  
49  
50  
51  
52  
53  
54  
55  
56  
57  
58  
59  
60

Figure 5 shows spectra representing the optimum transfer from the carbonyl carbon to the alpha carbon. All spectra are acquired with co-addition of 4 transients and identical receiver gain. The Rf amplitude for the cross-polarization step was  $\omega_1/2\pi = 200$  Hz. Figure 5(a) shows a standard pulse acquire with  $^1\text{H}$  decoupling during acquisition, i.e. no NOE enhancement. Figure 5(b) shows the spectrum following selective excitation of the carbonyl  $^{13}\text{C}$  with a 1ms Gaussian pulse. Figure 5(c) shows the spectrum following selective excitation of the carbonyl  $^{13}\text{C}$  followed by cross-polarization to the alpha  $^{13}\text{C}$ . The integrated signal in (c) is 91% that of the carbonyl signal after selective excitation in (b) and 88% that of the alpha carbon signal from direct excitation in (a).

## VII. CONCLUSION

We have demonstrated the use of homonuclear Hartmann-Hahn for achieving polarization transfer between two  $^{13}\text{C}$  nuclei that possess a mutual scalar coupling in solution state NMR. The method is capable of achieving at least a 90% transfer of polarization. With the advent of new DNP techniques this method may be a useful tool for extending the number of systems that are amenable to study using this technique.

## ACKNOWLEDGEMENTS

This work was supported by Cancer Research UK [CUK] grant number C1060/A5117 and by Basic Technology Programme grant number GR/S23612/01.

## REFERENCES

- [1] G. Frossati, *J. Low Temp. Phys.* **111**, 521 (1998).
- [2] A. Kastler, *J. Phys. Radium* **11**, 255 (1950).
- [3] W. Happer, E. Miron, D. Schreiber, W. A. van Wijngarden and X. Zeng, *Phys. Rev. A* **29**, 3092 (1984).
- [4] D. Raftery, H. Long, T. Meersmann, P. J. Grandinetti, L. Reven and A. Pines, *Phys. Rev. Lett.* **66**, 584 (1991).
- [5] C. R. Bowers and D. P. Weitekamp, *Phys. Rev. Lett.* **57**, 2645 (1986).
- [6] A. Abragam and M. Goldman: *Nuclear Magnetism: Order and Disorder*, Clarendon, Oxford, 1982.
- [7] C. P. Slichter: *Principles of Magnetic Resonance*, Springer-Verlag, Berlin, 1990.
- [8] J. H. Ardenkjaer-Larsen, B. Fridlund, A. Gram, G. Hansson, L. Hansson, M. H. Lerche, R. Servin, M. Thaning and K. Golman, *Proc. Natl. Acad. Sci. U. S. A.* **100**, 10158 (2003).
- [9] K. Golman, J. H. Ardenkjaer-Larsen, J. Stefan Petersson, S. Mansson and I. Leunbach, *Proc. Natl. Acad. Sci. U. S. A.* **100**, 10435 (2003).
- [10] K. Golman, R. i. t. Zandt and M. Thaning, *Proc. Natl. Acad. Sci. U. S. A.* **103**, 11270 (2006).
- [11] K. Golman, R. i. t. Zandt, M. H. Lerche, R. Pehrson and J. H. Ardenkjaer-Larsen, *Cancer Res.* **66**, 10855 (2006).
- [12] G. A. Morris and R. Freeman, *J. Am. Chem. Soc.* **101**, 760 (1979).
- [13] S. R. Hartmann and E. L. Hahn, *Phys. Rev.* **128**, 2042 (1962).
- [14] P. Pelupessy and E. Chiarparin, *Concepts Magn. Reson.* **12**, 103 (2000).
- [15] S. J. Glaser and J. J. Quant, *Adv. Magn. Opt. Reson.* **19**, 59 (1996).
- [16] T. R. Eykyn, D. J. Philp and P. W. Kuchel, *J. Chem. Phys.* **118**, 6997 (2003).
- [17] T. R. Eykyn, D. J. Philp and P. W. Kuchel, *Chem. Phys. Lett.* **376**, 732 (2003).
- [18] E. Chiarparin, P. Pelupessy, B. Cutting, T. R. Eykyn and G. Bodenhausen, *J. Biomol. NMR* **13**, 61 (1999).
- [19] R. Konrat, I. Burghardt and G. Bodenhausen, *J. Am. Chem. Soc.* **113**, 9135 (1991).
- [20] I.-Y. Choi, S.-P. Lee and J. Shen, *Magn. Reson. Med.* **53**, 503 (2005).
- [21] L. Emsley, I. Burghardt and G. Bodenhausen, *J. Magn. Reson.* **90**, 214 (1990).
- [22] J. Huth and G. Bodenhausen, *J. Magn. Reson. Ser. A* **114**, 129 (1995).

[23] E. Kupce and R. Freeman, *J. Magn. Reson. Ser. A* **112**, 261 (1995).

### FIGURE CAPTIONS

Figure 1. Coherence transfer functions calculated for an isolated  $^{13}\text{C}$  spin-pair under the influence of homonuclear Hartmann-Hahn. (a) Transfer functions for the source  $^{13}\text{C}$  coherences  $\langle S_{1x} \rangle$ , solid line, and  $\langle 2S_{1y}S_{2z} \rangle$ , dashed line. (b) The resulting build-up of polarization on spin 2  $\langle S_{2x} \rangle$ , solid line, and  $\langle 2S_{1z}S_{2y} \rangle$ , dashed-dotted line. Also displayed (c) and (d) are the same transfer functions calculated for a  $^{13}\text{C}$  spin-pair with an additional heteronuclear scalar coupling to  $^1\text{H}$ . Simulations were calculated employing the Hamiltonian in equation (4) with the scalar coupling constants set to  $^1J_{\text{CC}} = 50$  Hz,  $^1J_{\text{CH}} = 145$  Hz and  $^2J_{\text{CH}} = 10$  Hz. The spin-lock amplitude was set equal to the carbon-carbon coupling  $\omega_1/2\pi = 50$  Hz.

Figure 2. Simulated offset profile displaying the amplitude of the excited transverse magnetization  $(M_x^2 + M_y^2)^{1/2}$  for a 10ms cosine modulated pulse with a frequency offset of  $\Delta\Omega = 1000$  Hz. In (a) the RF amplitude was set to  $\omega_1/2\pi = 50$  Hz, i.e. much smaller than the offset whereas in (b) it was set equal to the offset  $\omega_1/2\pi = 1000$  Hz.

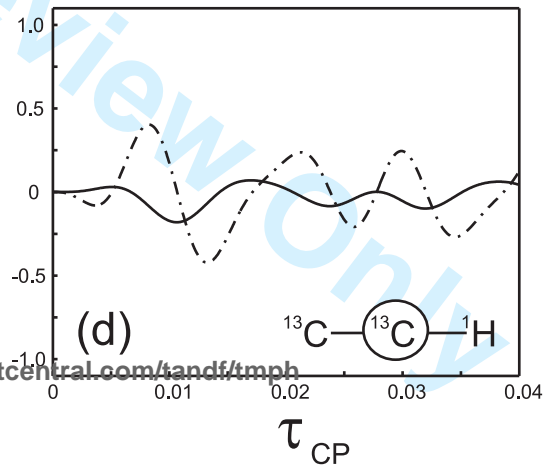
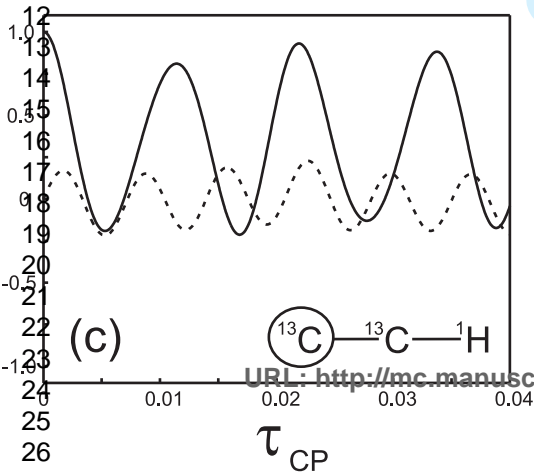
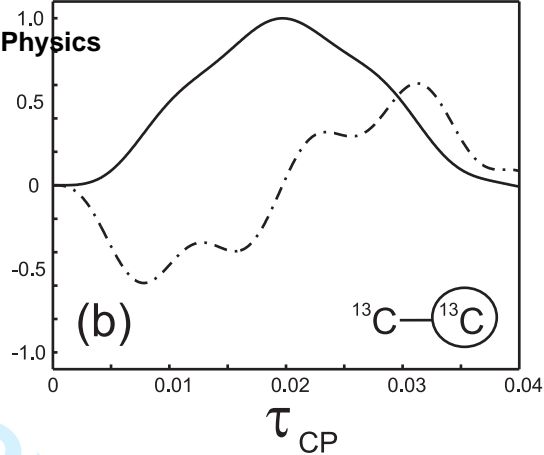
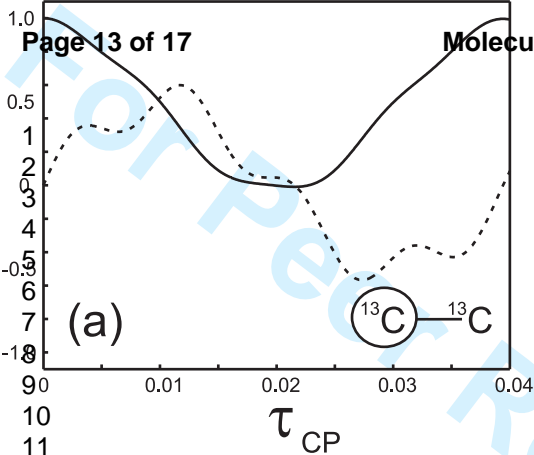
Figure 3. Pulse sequence for achieving magnetization transfer by homonuclear Hartmann-Hahn cross-polarization in solution state. The phase cycle was  $\phi_1 = \phi_{\text{rec}} = x, -x, x, -x$ . The phase of the amplitude modulated spin-lock was kept constant and applied with x phase.

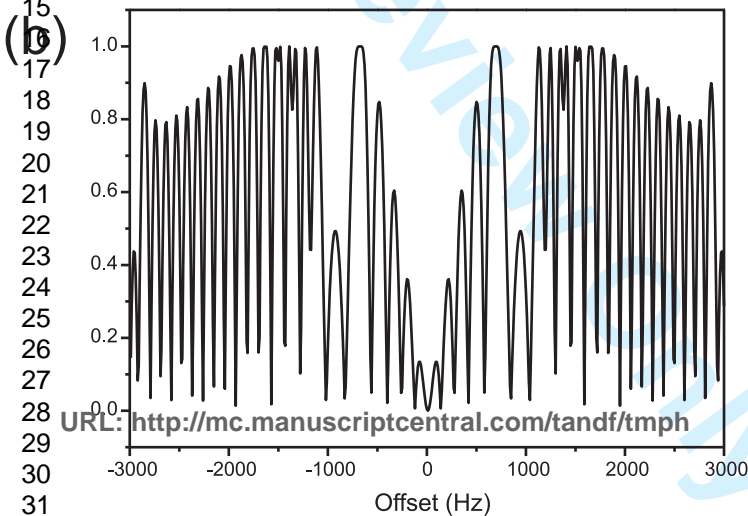
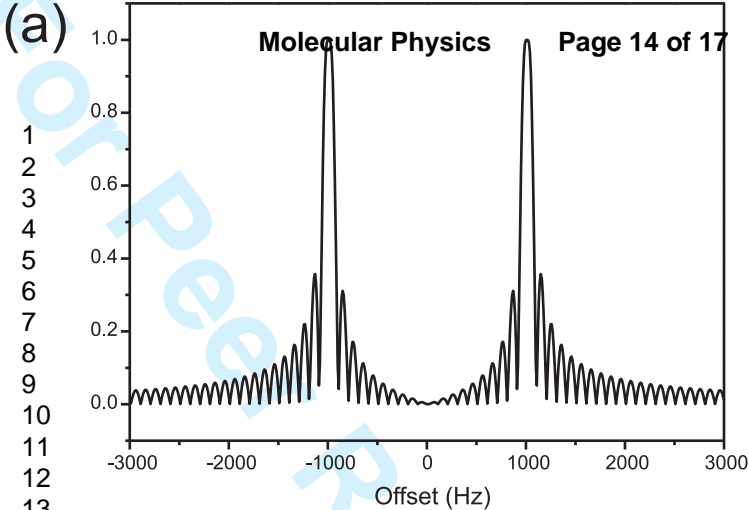
Figure 4. Transfer efficiency as a function of spin-lock amplitude. The vertical scale gives the integral of the alpha  $^{13}\text{C}$  magnetization following cross-polarization as a percentage of the initial carbonyl magnetization resulting from selective excitation. **The solid line is a third order polynomial fit to guide the eye.** An optimum transfer is observed for spin-lock amplitudes of the order  $\omega_1/2\pi = 200$  Hz.

Figure 5. (a)  $^{13}\text{C}$  spectrum employing standard pulse acquire with  $^1\text{H}$  decoupling during acquisition and no NOE enhancement. The inset shows an expanded view of the two peaks with a splitting of 53.5 Hz due to the  $^{13}\text{C}$ - $^{13}\text{C}$  scalar coupling. (b) Selective excitation of the carbonyl carbon employing a 1 ms Gaussian pulse. (c)

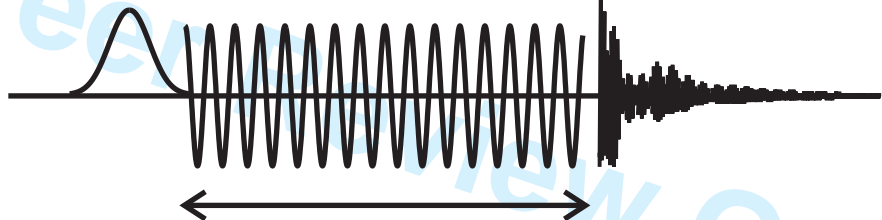
1  
2  
3 Selective excitation of the carbonyl carbon followed by cross-polarization to the alpha  
4 carbon. All spectra are displayed on the same scale with identical receiver gain and  
5  
6  
7 co-addition of 4 transients.  
8  
9  
10  
11  
12  
13  
14  
15  
16  
17  
18  
19  
20  
21  
22  
23  
24  
25  
26  
27  
28  
29  
30  
31  
32  
33  
34  
35  
36  
37  
38  
39  
40  
41  
42  
43  
44  
45  
46  
47  
48  
49  
50  
51  
52  
53  
54  
55  
56  
57  
58  
59  
60

For Peer Review Only



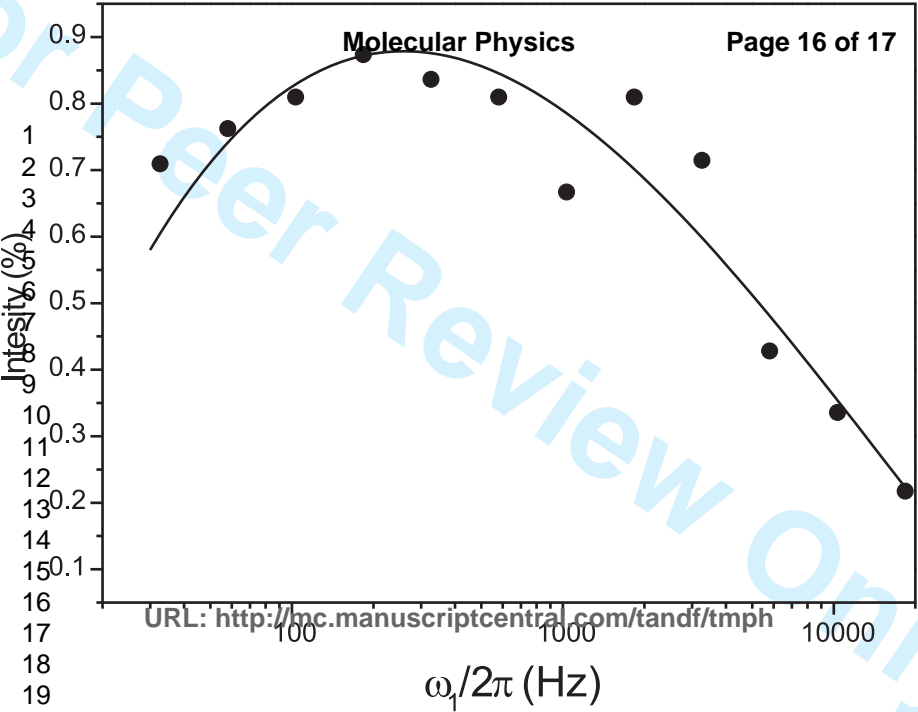




$\phi_1$  $\phi_{rec}$ 13  
2 CURL: <http://mc.manuscriptcentral.com/tandf/tmph>

WALTZ16

9  
10 H



URL: <http://mc.manuscriptcentral.com/tandf/tmph>

